Journal of Nuclear Materials 392 (2009) 525–530

Contents lists available at ScienceDirect

Journal of Nuclear Materials

journal homepage: www.elsevier.com/locate/jnucmat

Thermodynamic modeling of the Mg–Pu and Cu–Pu systems

C.P. Wang, W. Fang, Z.S. Li, X.J. Liu *

Department of Materials Science and Engineering, College of Materials, and Research Center of Materials Design and Applications, Xiamen University, Xiamen 361005, PR China

ARTICLE INFO

Article history:
Received 14 November 2008
Accepted 21 April 2009

PACS:
82.60.−s
81.30.Bx

ABSTRACT

The thermodynamic assessment of the Mg–Pu and Cu–Pu systems was carried out by using the calculation of phase diagrams (CALPHAD) method on the basis of experimental data including thermodynamic properties and phase equilibria. The Gibbs free energies of the liquid, fcc, hcp, αPu, βPu, γPu, δPu, δ′Pu, and εPu phases were described by the subregular solution model with a Redlich–Kister equation, and those of the intermetallic compounds in the Mg–Pu and Cu–Pu binary systems were described by the sublattice model. A consistent set of thermodynamic parameters were derived for describing the Gibbs free energies of solution phases and intermetallic compounds in the Mg–Pu and Cu–Pu binary systems. An agreement between the calculated results and experimental data is obtained.

1. Introduction

Metallic fuels have been recognized as an excellent alternative to conventional advanced fast reactor fuels due to high burn-up, favorable thermal response, and inherent safety characteristics [1]. A variety of Pu-based alloys have been tested as fuels for fast reactors in the United States and Europe with various degrees of success [2]. The phase diagrams are important for understanding the complex processes that may take place in a nuclear energy plant and helping us guide the selection and development of new metallic fuels.

Calculation of phase diagrams (CALPHAD) method is a powerful tool to cut down on cost and time during development of materials [3], effectively provides a clear guideline for materials design. Our goal is to develop a thermodynamic database of the phase diagrams in the nuclear materials. The present authors have made some thermodynamic assessments of the phase diagrams in the U, Th and Pu base alloy systems [4–11]. As a part of the thermodynamic database, the purpose of the present work is to carry out thermodynamic assessment in the Mg–Pu and Cu–Pu systems based on the CALPHAD method.

2. Thermodynamic models

Information on stable solid phases and the used models for the Mg–Pu and Cu–Pu systems [12] is listed in Table 1.

2.1. Gas phases

The gas phase is described as an ideal mixture containing the gaseous species Mg, Mg_2 and Pu. The Gibbs free energy of the species in the gas phase is given as:

$$G^{\text{gas}} = \sum_i x_i {}^0G_i^{\text{gas}} + RT\sum_i x_i \ln x_i + RT\ln\left(\frac{P}{P_0}\right), \tag{1}$$

where x_i is the mole fraction of the specie in gas phase, ${}^0G_i^{\text{gas}}$ is the standard Gibbs free energy of the gaseous species i, which is taken from the SGTE pure element database [13], R the gas constant, and P_0 the standard pressure at 1 bar.

2.2. Solution phase

The Gibbs free energies of the solution phases in the Me–Pu (Me: Mg, Cu) system were described by the subregular solution model [14], and the molar Gibbs free energy for each solution phase is described as follows:

$$G_m^{\phi} = x_{Me}{}^0G_{Me}^{\phi} + x_{Pu}{}^0G_{Pu}^{\phi} + RT(x_{Me}\ln x_{Me} + x_{Pu}\ln x_{Pu}) + x_{Me}x_{Pu}\sum_{m=0}^{n} {}^mL_{Me,Pu}^{\phi}(x_{Me}-x_{Pu})^m, \tag{2}$$

where ${}^0G_{Me}^{\phi}$ and ${}^0G_{Pu}^{\phi}$ are the molar Gibbs free energies of pure elements Me and Pu in the ϕ phase, which is taken from the compilation by Dinsdale [15]. x_{Me} and x_{Pu} are the mole fractions of Me and Pu components, and ${}^mL_{Me,Pu}^{\phi}$ is the binary interaction parameter between Me and Pu atoms, which is expressed as:

$${}^mL_{Me,Pu}^{\phi} = a + bT, \tag{3}$$

where the parameters of a and b were evaluated based on the available experimental data in the present work.

* Corresponding author. Tel.: +86 592 2187888; fax: +86 592 2187966.
E-mail address: lxj@xmu.edu.cn (X.J. Liu).

0022-3115/$ - see front matter © 2009 Elsevier B.V. All rights reserved.
doi:10.1016/j.jnucmat.2009.04.017

Table 1
Stable solid phases and models used for the Mg–Pu and Cu–Pu systems.

System	Phase	Prototype	Struckturbericht designation	Modeling phase	Used models
Mg–Pu	εPu	W	A2	(Mg,Pu)	Subregular solution model
	δ′Pu	In	A6	(Mg,Pu)	Subregular solution model
	δPu	Cu	A1	(Mg,Pu)	Subregular solution model
	γPu	γPu	–	(Mg,Pu)	Subregular solution model
	βPu	βPu	–	(Mg,Pu)	Subregular solution model
	αPu	αPu	–	(Mg,Pu)	Subregular solution model
	(Mg)	Mg	A3	(Mg,Pu)	Subregular solution model
	Mg_6Pu	–	–	$(Mg)_6(Pu)$	Two-sublattice model
	Mg_4Pu	–	–	$(Mg)_4(Pu)$	Two-sublattice model
	Mg_2Pu	CaF_2	C1	$(Mg)_2(Pu)$	Two-sublattice model
Cu–Pu	εPu	W	A2	(Cu,Pu)	Subregular solution model
	δ′Pu	In	A6	(Cu,Pu)	Subregular solution model
	δPu	Cu	A1	(Cu,Pu)	Subregular solution model
	γPu	γPu	–	(Cu,Pu)	Subregular solution model
	βPu	βPu	–	(Cu,Pu)	Subregular solution model
	αPu	αPu	–	(Cu,Pu)	Subregular solution model
	(Cu)	Cu	A1	(Cu,Pu)	Subregular solution model
	Cu_6Pu	$CeCu_6$	–	$(Cu)_6(Pu)$	Two-sublattice model
	$Cu_{17}Pu_4$	–	–	$(Cu)_{17}(Pu)_4$	Two-sublattice model
	Cu_4Pu	–	–	$(Cu)_4(Pu)$	Two-sublattice model
	Cu_2Pu	$CeCu_2$	–	$(Cu)_2(Pu)$	Two-sublattice model

2.3. Stoichiometric intermetallic compounds

The compounds of the Mg_6Pu, Mg_4Pu and Mg_2Pu in the Mg–Pu system and Cu_6Pu, $Cu_{17}Pu_4$, Cu_4Pu and Cu_2Pu in the Cu–Pu system are treated as stoichiometric phases. The Gibbs free energy per mole of formula unit for Me_mPu_n (Me: Mg, Cu) can be expressed by the two-sublattice model [16] as follows:

$$\Delta G_f^{Me_mPu_n} = {}^0G_m^{Me_mPu_n} - m{}^0G_{Me}^{ref} - n{}^0G_{Pu}^{ref} = a' + b'T, \quad (4)$$

where $\delta G_f^{Me_mPu_n}$ denotes the standard Gibbs free energy of formation of the stoichiometric compound from pure elements, ${}^0G_{Me}^{ref}$ and ${}^0G_{Pu}^{ref}$ are the molar Gibbs free energies of the pure elements Me and Pu. The parameters of a' and b' are evaluated in the present optimization.

3. Experimental information

3.1. The Mg–Pu system

The phase diagram of the Mg–Pu system consists of a miscibility gap in the liquid phase, seven solid solution phases (αPu, βPu, γPu, δPu, δ′Pu, εPu, and (Mg)), and three intermetallic compounds ($PuMg_6$, $PuMg_4$ and $PuMg_2$). Many researchers [17–19] have investigated the miscibility gap of the liquid phase in the Mg–Pu system. Schonfeld et al. [17] initially reported a large region of liquid immiscibility in the Mg–Pu system. Schilb and Steunenberh [18] concluded that the liquid miscibility gap ranges from 16 to 91.6 at.% Pu at 625 °C, which is in agreement with the tentative diagram by Schonfeld et al. [17]. Knoch et al. [19] found that this miscibility gap extends from ~9.8 to ~99.5 at.% Pu at 638 °C. The solid solubility of Pu in (Mg) determined by Hodkin and Mardon [20] is about 2.2 at.% at 475 °C. Ellinger et al. [21] pointed out that there is no significant solid solubility of Mg in Pu in their construction of the binary phase diagram. Knoch et al. [19] mentioned that the solid solubility of Mg in Pu is less than 0.5 at.%. Coffinberry and Ellinger [22] reported a $PuMg_2$ intermetallic compound according to their investigation.

Later, Axler et al. [23] determined the phase diagram in the Mg–Pu binary system using metallography, electron microprobe, X-ray diffraction (XRD) and differential thermal analysis (DTA), where the temperature (553 ± 3 °C) of the $L_1 \leftrightarrow (Mg) + \varepsilon Pu$ eutectic reaction is consistent with that (550 °C) determined by Schonfeld et al. [17], and the eutectic composition (6.5 at.% Pu) is more reasonable from a thermodynamic viewpoint. Axler et al. [23] also calculated phase equilibria in relation with the gas phase in the Mg–Pu binary system. Okamoto [12] reviewed the phase diagram in the Mg–Pu system based mainly on experimental data [23], as shown in Fig. 1.

The Gibbs free energies and enthalpies of formation of the liquid phase at 927 °C were determined by Knoch et al. [19] and Axler et al. [23] on the basis of electromagnetic fields (EMF) measurements.

3.2. The Cu–Pu system

The Cu–Pu phase diagram consists of the terminal phase (Cu) with negligible solubility of Pu, four intermetallic compounds (Cu_6Pu, $Cu_{17}Pu_4$, Cu_4Pu and Cu_2Pu), and the terminal phase (Pu) with a maximum solubility of ~3 at.% Cu. The Cu–Pu phase diagram was subsequently investigated by Bochvar et al. [24], Schonfeld et al. [25], Rhinehammer et al. [26] and Kutaitsev et al. [27]. Although Bochvar et al. [24] published a phase diagram in this system, a description of the experimental techniques was not

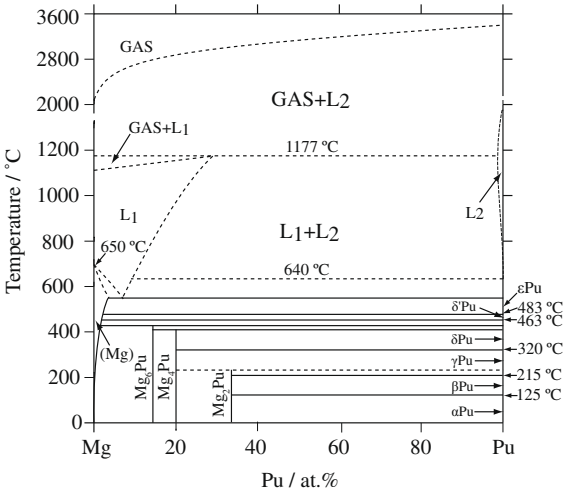

Fig. 1. Mg–Pu phase diagram reviewed by Okamoto [12].

reported. Schonfeld et al. [25] reported the existence of the Cu_7Pu, Cu_3Pu and Cu_2Pu compounds. Rhinehammer et al. [26] conducted a detailed investigation of the Cu–Pu phase diagram using DTA technique with heating and cooling rates of 1–3 °C/min, and confirmed the existence of the Cu_4Pu, Cu_2Pu, $Cu_{17}Pu_4$, and $Cu_{11}Pu_2$ compounds. However, according to subsequent research by Wittenberg and Groce [28], the existence of the Cu_6Pu compound instead of the $Cu_{11}Pu_2$ compound was confirmed. Kutaitsev et al. [27] studied the phase diagram in the Cu–Pu system by DTA, dilatometry, XRD and metallography. Three eutectic reactions, namely $L \leftrightarrow Cu_2Pu + \varepsilon Pu$, $L \leftrightarrow Cu_4Pu + Cu_2Pu$ and $L \leftrightarrow Cu + Cu_6Pu$, were respectively reported by Rhinehammer et al. [26] and Kutaitsev et al. [27]. Subramanian [29] reviewed the Cu–Pu binary phase diagram based on experimental data [26,27], as shown in Fig. 2.

In addition, Miedema [30] predicted the enthalpies of formation of the Pu_4Cu_2, $PuCu_4$ and $PuCu_6$ intermetallic compounds at 298 K.

4. Optimized results and discussion

The optimization of the thermodynamic parameters was carried out by using the PARROT [31] program in the Thermo-Calc software [32], which can handle various kinds of experimental data.

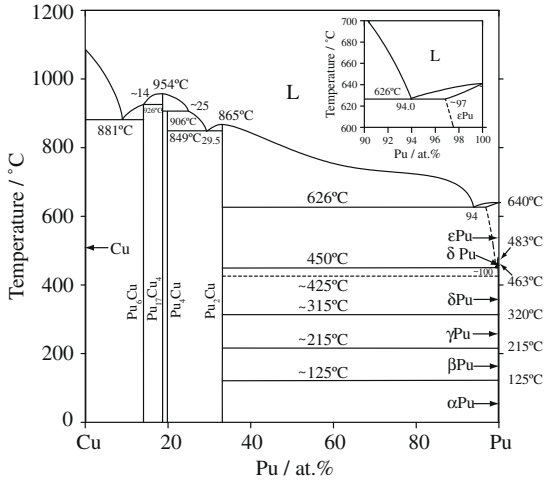

Fig. 2. Cu–Pu phase diagram reviewed by Subramanian [29].

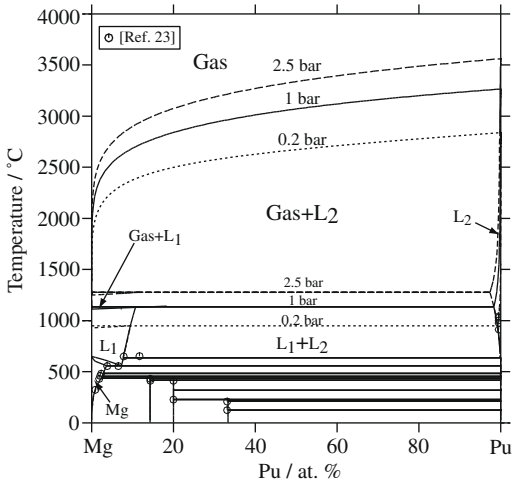

Fig. 3. Calculated Mg–Pu phase diagram as a function of pressure compared with experimental data [23].

The procedure involves a weighted least-square optimization of the model parameters based on the experimental information on thermodynamic properties and phase diagram. Each piece of selected information was given a certain weight based on the importance of the data, and was modified by trial and error during the assessment, until most of the selected experimental information was reproduced within the expected uncertainty limits.

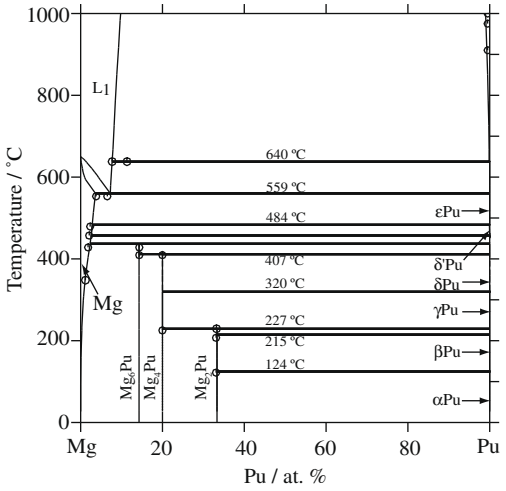

Fig. 4. Enlarged part of the calculated Mg–Pu phase diagram.

Table 2
Thermodynamic parameters for the Mg–Pu system optimized in this work.

Parameters in each phase (J/mol)
Liquid phase, format (Mg,Pu)$_1$
${}^0L^{\mathrm{Liq}}_{\mathrm{Mg,Pu}} = 51100 - 3.5T$
${}^1L^{\mathrm{Liq}}_{\mathrm{Mg,Pu}} = -34500 + 13.1T$
${}^2L^{\mathrm{Liq}}_{\mathrm{Mg,Pu}} = -30600 + 10.5T$
εPu phase, format (Mg,Pu)$_1$
${}^0L^{\varepsilon\mathrm{Pu}}_{\mathrm{Mg,Pu}} = 58000$
δ'Pu phase, format (Mg,Pu)$_1$
$G^{\delta'\mathrm{Pu}}_{\mathrm{Mg}} = 1000 + G^{\mathrm{hcp}}_{\mathrm{Mg}}$
${}^0L^{\delta'\mathrm{Pu}}_{\mathrm{Mg,Pu}} = 48000$
δPu phase, format (Mg,Pu)$_1$
${}^0L^{\delta\mathrm{Pu}}_{\mathrm{Mg,Pu}} = 50000$
γPu phase, format (Mg,Pu)$_1$
$G^{\gamma\mathrm{Pu}}_{\mathrm{Mg}} = 5000 + G^{\mathrm{hcp}}_{\mathrm{Mg}}$
${}^0L^{\gamma\mathrm{Pu}}_{\mathrm{Mg,Pu}} = 50000$
βPu phase, format (Mg,Pu)$_1$
$G^{\beta\mathrm{Pu}}_{\mathrm{Mg}} = 25000 + G^{\mathrm{hcp}}_{\mathrm{Mg}}$
${}^0L^{\beta\mathrm{Pu}}_{\mathrm{Mg,Pu}} = 50000$
αPu phase, format (Mg,Pu)$_1$
$G^{\alpha\mathrm{Pu}}_{\mathrm{Mg}} = 5000 + G^{\mathrm{hcp}}_{\mathrm{Mg}}$
${}^0L^{\alpha\mathrm{Pu}}_{\mathrm{Mg,Pu}} = 30000$
hcp phase, format (Mg,Pu)$_1$
$G^{\mathrm{hcp}}_{\mathrm{Pu}} = 5000 + G^{\alpha\mathrm{Pu}}_{\mathrm{Pu}}$
${}^0L^{\mathrm{hcp}}_{\mathrm{Mg,Pu}} = 15000$
$PuMg_6$ phase, format $(Pu)_{0.1429}(Mg)_{0.8571}$
$G^{\mathrm{PuMg_6}}_{\mathrm{Pu:Mg}} = 0.1429G^{\alpha\mathrm{Pu}}_{\mathrm{Pu}} + 0.8571G^{\mathrm{hcp}}_{\mathrm{Mg}} - 900 + 0.54T$
$PuMg_4$ phase, format $(Pu)_{0.2}(Mg)_{0.8}$
$G^{\mathrm{PuMg_4}}_{\mathrm{Pu:Mg}} = 0.2G^{\alpha\mathrm{Pu}}_{\mathrm{Pu}} + 0.8G^{\mathrm{hcp}}_{\mathrm{Mg}} - 1000 + 0.485T$
$PuMg_2$ phase, format $(Pu)_{0.3333}(Mg)_{0.6667}$
$G^{\mathrm{PuMg_2}}_{\mathrm{Pu:Mg}} = 0.3333G^{\alpha\mathrm{Pu}}_{\mathrm{Pu}} + 0.6667G^{\mathrm{hcp}}_{\mathrm{Mg}} - 1000 + 0.42T$

Table 3
Calculated invariant reactions in the Mg–Pu system with experimental data.

Reaction type	Reaction	Pu (at.%)			T (°C)	References
Peritectoid	$Mg_4Pu + \gamma Pu \rightarrow Mg_2Pu$	20	100	33.3	225	[23]
		20	100	33.3	227	This work
Peritectoid	$Mg_6Pu + \delta Pu \rightarrow Mg_4Pu$	14.3	100	20	407	[23]
		14.3	100	20	407	This work
Peritectoid	$(Mg) + \delta Pu \rightarrow Mg_6Pu$	2.0	100	14.3	438	[23]
		2.1	100	14.3	437	This work
Eutectic	$L_1 \rightarrow (Mg) + \varepsilon Pu$	6.5	3.8	100	556	[23]
		6.9	3.7	100	559	This work
Monotectic	$L_2 \rightarrow L_1 + \varepsilon Pu$	99.5	–	100	640	[23]
		99.5	7.7	100	640	This work
–	$L_2 + gas \rightarrow L_1$	99.3	0	10.7	1143	This work

4.1. The Mg–Pu system

The calculated phase diagram and the enlarged part of the Mg–Pu system compared with all experimental data are shown in Figs. 3 and 4, respectively. It can be seen that the calculated results are in agreement with the experimental data [23]. The calculated solid solubility of Mg in Pu is less than 0.5 at.%, which is in agreement with that reported by Knoch et al. [19]. In addition, the gas phase in the Mg–Pu system under different pressures (0.2, 1 and 2.5 bar) is calculated based on the ideal gas model, where the effect of pressure on solid phases is not considered in the process of assessment, as shown in Fig. 3. It can be seen that the boiling point increases and the two-phase region (gas + liquid) becomes larger with the increasing of the pressure.

A complete set of the thermodynamic parameters describing the Gibbs free energy of each phase in this system is given in Table 2. And all invariant reactions and special points in the Mg–Pu system are summarized in Table 3 with the experimental data [23] for comparison.

The calculated Gibbs free energy and enthalpy of formation of the liquid phase at 927 °C are shown in Figs. 5 and 6, respectively. It can be seen that the calculated results are in agreement with the experimental data [19,23].

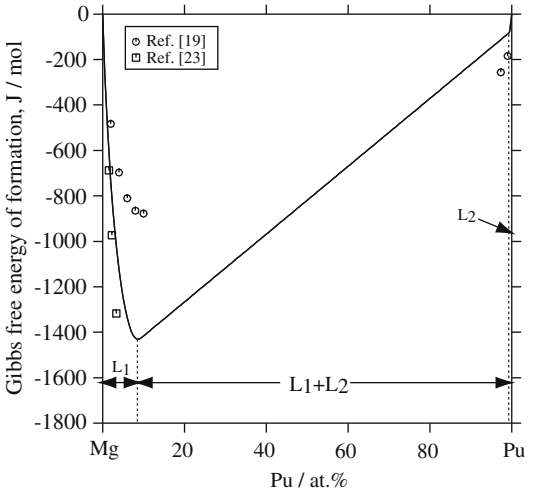

Fig. 5. Calculated Gibbs free energy of the liquid phase at 927 °C in the Mg–Pu system compared with experimental data [19,23] (reference states: liquid (Pu) phase and liquid (Mg) phase).

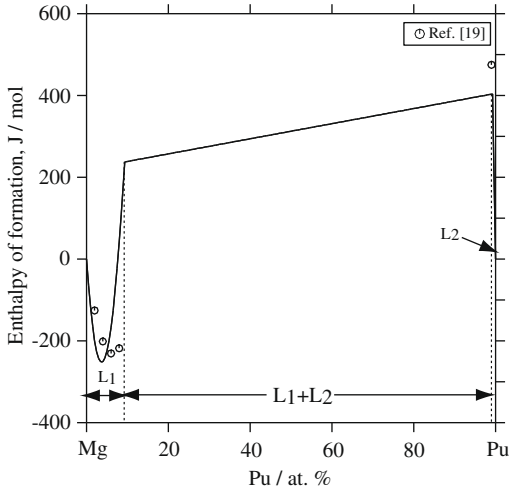

Fig. 6. Calculated enthalpy of formation of the liquid phase at 927 °C in the Mg–Pu system compared with experimental data [19] (reference states: liquid (Pu) phase and liquid (Mg) phase).

4.2. The Cu–Pu system

The calculated Cu–Pu phase diagram together with the experimental data [26,27] is shown in Fig. 7. It is seen that the calculated results are in agreement with the experimental data [26], except for the temperature of the $L \rightarrow Cu_4Pu + Cu_2Pu$ eutectic reaction. The calculated temperature of this eutectic reaction is 857 °C, however, Rhinehammer et al. [26] reported this eutectic temperature to be 849 °C, and Kutaitsev et al. [27] gave an estimated value (857 °C). Thus, the calculated eutectic temperature can be accepted. A set of complete self-consistent thermodynamic

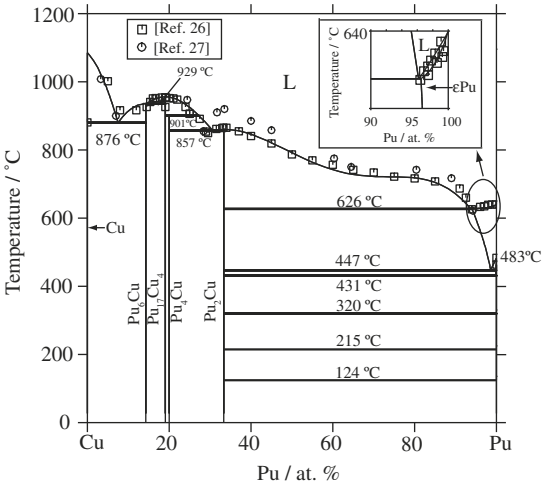

Fig. 7. Calculated Cu–Pu phase diagram compared with experimental data [26,27].

parameters describing the Gibbs free energy of each phase in the Cu–Pu system are given in Table 4, and the calculated compositions and temperatures for the invariant reactions compared with the experimental data [26] are listed in Table 5.

The calculated enthalpies of formation of $PuCu_2$, $PuCu_4$ and $PuCu_6$ at 298 K are compared with the data predicted by Miedema [30] in Fig. 8, where the reference states are fcc Cu and αPu, respectively. It can be seen that the calculated enthalpy of formation of $PuCu_2$ is in good agreement with the data predicted by Miedema [30]. For the $PuCu_4$ and $PuCu_6$ intermetallic compounds, although the calculated enthalpies of formation are higher than Miedema's values [30], they are still acceptable by considering the inaccuracy associated with Miedema's estimated values.

Table 4
Thermodynamic parameters for the Cu–Pu system optimized in this work.

Parameters in each phase (J/mol)
Liquid phase, format (Cu,Pu)$_1$
${}^0L^{Liq}_{Cu,Pu} = -47000 - 25T$
${}^1L^{Liq}_{Cu,Pu} = -76000 + 12.5T$
${}^2L^{Liq}_{Cu,Pu} = 3000 - 18T$
${}^3L^{Liq}_{Cu,Pu} = 20000$
εPu phase, format (Cu,Pu)$_1$
${}^0L^{\varepsilon Pu}_{Cu,Pu} = -20000 - 10T$
${}^1L^{\varepsilon Pu}_{Cu,Pu} = 8500 - 3T$
δ′Pu phase, format (Cu,Pu)$_1$
$G^{\delta' Pu}_{Cu} = 4000 + G^{fcc}_{Cu}$
${}^0L^{\delta' Pu}_{Cu,Pu} = -13000 - 7T$
δPu phase, format (Cu,Pu)$_1$
${}^0L^{\delta Pu}_{Cu,Pu} = 51000$
γPu phase, format (Cu,Pu)$_1$
$G^{\gamma Pu}_{Cu} = 4000 + G^{fcc}_{Cu}$
${}^0L^{\gamma Pu}_{Cu,Pu} = 43000$
βPu phase, format (Cu,Pu)$_1$
$G^{\beta Pu}_{Cu} = 1000 + G^{fcc}_{Cu}$
${}^0L^{\beta Pu}_{Cu,Pu} = 40000$
αPu phase, format (Cu,Pu)$_1$
$G^{\alpha Pu}_{Cu} = 2000 + G^{fcc}_{Cu}$
${}^0L^{\alpha Pu}_{Cu,Pu} = 60000$
Cu_6Pu, phase, format $(Cu)_{0.8571}(Pu)_{0.1429}$
$G^{Cu_6Pu}_{Cu:Pu} = 0.8571G^{fcc}_{Cu} + 0.1429G^{\alpha Pu}_{Pu} - 26400 + 6.08T$
$Cu_{17}Pu_4$, phase, format $(Cu)_{0.8095}(Pu)_{0.1905}$
$G^{Cu_{17}Pu_4}_{Cu:Pu} = 0.8095G^{fcc}_{Cu} + 0.1905G^{\alpha Pu}_{Pu} - 32660 + 7.2T$
Cu_4Pu phase, format $(Cu)_{0.8}(Pu)_{0.2}$
$G^{Cu_4Pu}_{Cu:Pu} = 0.8G^{fcc}_{Cu} + 0.2G^{\alpha Pu}_{Pu} - 34000 + 8.0T$
Cu_2Pu phase, format $(Cu)_{0.6667}(Pu)_{0.3333}$
$G^{Cu_2Pu}_{Cu:Pu} = 0.6667G^{fcc}_{Cu} + 0.3333G^{\alpha Pu}_{Pu} - 52700 + 21.20T$

Table 5
Calculated invariant reactions in the Cu–Pu system with experimental data.

Reaction type	Reaction	Pu (at.%)			T (°C)	Reference
Eutectoid	δ′Pu → Cu_2Pu + δPu	~100	33.3	100	~425	[26]
		99.5	33.3	100	431	This work
Eutectoid	εPu → Cu_2Pu + δ′Pu	97.0	33.3	100	450	[26]
		98.0	33.3	100	447	This work
Eutectic	L → Cu_2Pu + εPu	94.0	33.3	97	626	[26]
		94.0	33.3	95.5	626	This work
Eutectic	L → Cu_4Pu + Cu_2Pu	29.5	20.0	33.3	849	[26]
		30.6	20.0	33.3	857	This work
Eutectic	L → (Cu) + Cu_6Pu	9.0	0	14.3	881	[26]
		7.9	0	14.3	876	This work
Peritectic	L + $Cu_{17}Pu_4$ → Cu_6Pu	~14	19.1	14.3	926	[26]
		14	19.1	14.3	929	This work
Peritectic	$Cu_{17}Pu_4$ + L → Cu_4Pu	19.1	~25	20.0	906	[26]
		19.1	26.5	20.0	901	This work

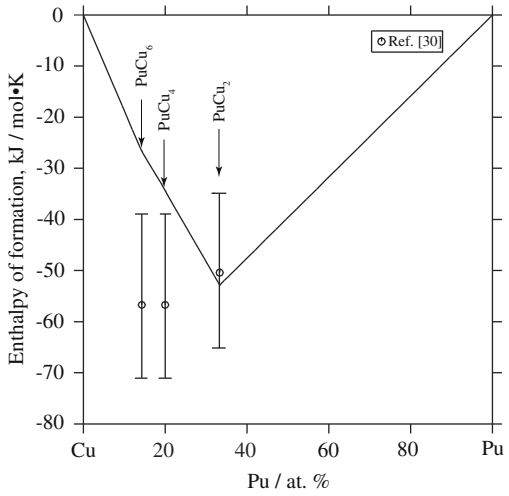

Fig. 8. Calculated enthalpies of formation of $PuCu_2$, $PuCu_4$ and $PuCu_6$ at 25 °C in the Cu–Pu system compared with the data predicted by Miedema [30] (reference states: fcc (Cu) phase and αPu phase).

5. Conclusions

The phase diagrams and thermodynamic properties of the Mg–Pu and Cu–Pu binary systems were evaluated by combining the thermodynamic models with available experimental information. A consistent set of optimized thermodynamic parameters has been derived for describing the Gibbs free energy of each solution phase and intermetallic compound in the Mg–Pu and Cu–Pu binary systems, and good agreement between the calculated results and most experimental data has been achieved.

Acknowledgements

This work was supported by the National Natural Science Foundation of China (Nos. 50425101 and 50771087).

References

[1] J.H. Kittel, B.R.T. Frost, J.P. Mustelier, K.Q. Bagley, G.C. Crittenden, J. Van dievoe, J. Nucl. Mater. 204 (1993) 1.
[2] S.S. Hecker, M. Stan, J. Nucl. Mater. 383 (2008) 112.
[3] L. Kaufman, H. Bernstein, Computer Calculation of Phase Diagram, Academic Press, New York, 1970.
[4] J. Wang, C.P. Wang, J. Nucl. Mater. 374 (1&2) (2008) 79.
[5] C.P. Wang, P. Yu, X.J. Liu, I. Ohnuma, R. Kainuma, J. Alloys Compd. 475 (1&2) (2008) 150.
[6] J. Wang, C.P. Wang, X.J. Liu, J. Nucl. Mater. 380 (1–3) (2008) 105.
[7] X.J. Liu, Z.S. Li, J. Wang, C.P. Wang, J. Nucl. Mater. 380 (1–3) (2008) 99.
[8] C.P. Wang, Y.F. Li, X.J. Liu, I. Ohnuma, R. Kainuma, J. Alloys Compd. 458 (1&2) (2008) 208.
[9] P.E.A. Turchi, L. Kaufman, S.H. Zhou, Z.K. Liu, J. Alloys Compd. 445 (2007) 28.
[10] M. Kurata, T. Ogata, K. Nakamura, T. Ogawa, J. Alloys Compd. 271 (1998) 640.
[11] M. Kurata, K. Nakamura, T. Ogata, J. Nucl. Mater. 294 (1&2) (2001) 123.
[12] H. Okamoto, Desk Handbook—Phase Diagrams for Binary Alloys, ASM International, 2000.
[13] The SGTE Substance Database, Version 1997, SGTE (Scientific Group Thermodata Europe), Grenoble, France, 1997.
[14] H.K. Hardy, Acta Metall. 1 (1953) 202.
[15] A.T. Dinsdale, CALPHAD 15 (1991) 317.
[16] M. Hillert, L.I. Stafansson, Acta Chem. Scand. 24 (1970) 3618.
[17] F.W. Schonfeld, E.M. Cramer, W.N. Miner, F.H. Ellinger, A.S. Coffinberry, Metall. Fuels 2 (1959) 587.
[18] J.D. Schilb, R.K. Steunenberh, Argonne National Laboratory, USA, Report ANL-6925, 1965, p. 48.
[19] W. Knoch, J.B. Knighton, R.K. Steunenberg, Nuc. Metall. 15 (1969) 535.
[20] D.J. Hodkin, P.G. Mardon, J. Nucl. Mater. 16 (1965) 271.

[21] F.H. Ellinger, W.N. Miner, D.R. O'Boyle, F.W Schonfeld, Los Alamos National Laboratory, USA, Report LA-3870, 1969, p. 59.
[22] A.S. Coffinberry, F.H. Ellinger, in: Proceedings of International Conference on the Peaceful Uses of Atomic Energy, vol. 9, 1956, p. 138.
[23] K.M. Axler, E.M. Foltyn, D.E. Peterson, R.I. Sheldon, W.B. Hutchinson, J. Nucl. Mater. 161 (1989) 132.
[24] A.A. Bochvar, S.T. Konobeevsky, V.I. Kutaitsev, T.S. Menshikova, N.T. Chebotarev, in: Proceedings of Second United Nations International Conference on Peaceful Uses Atomic Energy, Geneva, vol. 6, 1958, p. 184.
[25] F.W. Schonfeld, E.M. Cramer, W.N. Miner, F.H. Ellinger, A.S. Coffinberry, Metall. Fuels 2 (1959) 579.
[26] T.B. Rhinehammer, D.E. Etter, L.V. Jones, Plutonium 1960, in: E. Grison, W.B.H. Lord, R.D. Fowler (Eds.), Cleaver-Hume, London, 1961.
[27] V.I. Kutaitsev, N.T. Chebotarev, I.G. Lebedev, M.A. Andrianov, V.N. Konev, T.S. Menshikova, in: A.E. Kay, M.B. Waldron (Eds.), Proceedings of Third International Conference on Plutonium, Chapman and Hall, London, 1967.
[28] L.J. Wittenberg, G.R. Groce, Reactor Fuels and Materials Development Plutonium Research, 1964 Annual Report, MLM-1244, 1964.
[29] P.R. Subramanian, Phase Diagrams of Binary Copper Alloys, ASM International, 1994.
[30] A.R. Miedema, Plutonium 1975 and Other Actinides, in: H. Blank, R. Lindner (Eds.), North Holland, New York, 1976.
[31] B. Jansson, PhD Thesis, Division of Physical Metallurgy, Royal Institute of Technology, Stockholm, Sweden, 1984.
[32] B. Sundman, B. Jansson, J.O. Andersson, CALPHAD 9 (1985) 153.